Fig. 9 Representative MRM chromatograms of He-dG (A), He-dA (C), He-dC (E) and each [^{15}N]-labeled stable isotope (B, D, and F) in the kidneys of Alz-treated F344 *gpt* delta rats.

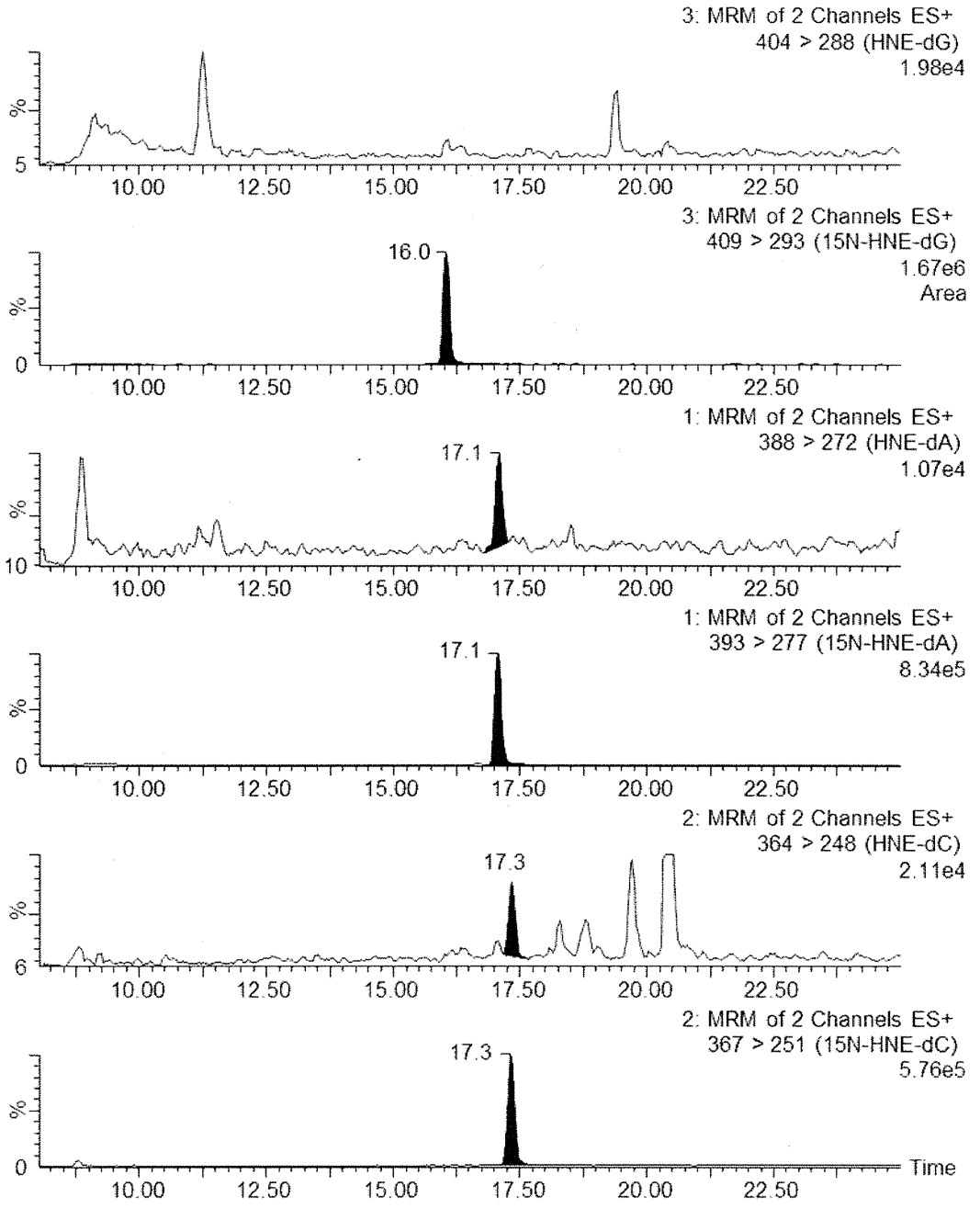

Table 1 Final body and organ weights

Item/group	Control	ES	MEG	EG
No. of animals	5	5	5	5
Body weight (g)	221.5 ± 14.7	182.1 ± 14.0**	215.6 ± 17.0	214.5 ± 10.3
Absolute weight (g)				
Liver	8.14 ± 0.78	7.45 ± 0.78	8.63 ± 1.18	8.85 ± 0.75
Kidney	1.46 ± 0.08	1.31 ± 0.05*	1.52 ± 0.11	1.58 ± 0.04
Relative weight (g/100g b.w.)				
Liver	3.67 ± 0.18	4.09 ± 0.13**	3.99 ± 0.25	4.12 ± 0.18**
Kidney	0.66 ± 0.02	0.72 ± 0.04*	0.71 ± 0.01	0.74 ± 0.05**

*, **: $p < 0.05, 0.01$ vs. Control group

Table 2 Summary of DNA adductome analysis

Compound	Organ	Peak No.	m/z	Retention time (min)	Peak area	Putative adducts	Ionized type
ES	Liver	I'	436	15.9	4309287	ES-3'-N^2-dG	$[M+Na]^+$
		II'	436	15.6	1037915	ES-1'-N^2-dG	$[M+Na]^+$
		I	414	15.9	4309287	ES-3'-N^2-dG	$[M+H]^+$
		II	414	15.6	1037915	ES-1'-N^2-dG	$[M+H]^+$
		III	414	15.3	27796	ES-3'-C8-dG	$[M+H]^+$
		IV	414	12.9	27796	ES-modified dG	$[M+H]^+$
		V	398	17.7	2234616	ES-3'-N^6-dA	$[M+H]^+$
		VI	374	15.2	28487	ES-modified dC	$[M+H]^+$
	Kidney	I'	436	15.9	4193	ES-3'-N^2-dG	$[M+Na]^+$
		II'	436	15.6	2898	ES-1'-N^2-dG	$[M+Na]^+$
		I	414	15.9	23402	ES-3'-N^2-dG	$[M+H]^+$
		II	414	15.6	36289	ES-1'-N^2-dG	$[M+H]^+$
		III	414	15.3	3393	ES-3'-C8-dG	$[M+H]^+$
		IV	414	12.9	1309	ES-modified dG	$[M+H]^+$
		V	398	17.7	13859	ES-3'-N^6-dA	$[M+H]^+$
		VI	374	15.2	1977	ES-modified dC	$[M+H]^+$
MEG	Liver	I'	466	14.6	2273268	MEG-modified dG	$[M+Na]^+$
		I	444	14.6	2273268	MEG-3'-N^2-dG	$[M+H]^+$
		II	428	16.3	354471	MEG-3'-N^6-dA	$[M+H]^+$
		III	404	13.8	11962	MEG-modified dC	$[M+H]^+$
	Kidney	I	444	14.6	16584	MEG-3'-N^2-dG	$[M+H]^+$
		II	428	16.3	4299	MEG-3'-N^6-dA	$[M+H]^+$
EG	Liver	N.D.					
	Kidney	N.D.					

Table 3 *gpt* MFs in the livers of *gpt* delta rats treated with ES, MEG and EG for 4 weeks

Treatment	Animal No.	Cm^R colonies (x 10^5)	6-TG^R and Cm^R colonies	Mutant frequency (x 10^{-5})	Mean±SD
Control	1	1.13	8	0.71	0.95 ± 0.28
	2	6.4	9	1.41	
	3	12.2	9	0.74	
	4	8.7	8	0.92	
	5	6.1	6	0.98	
ES	6	7.0	43	6.16	6.70 ± 0.86**
	7	3.4	22	6.52	
	8	1.3	10	7.94	
	9	2.8	16	5.73	
	10	4.8	34	7.13	
MEG	11	5.4	16	2.94	3.31 ± 2.02 *
	12	2.1	14	6.62	
	13	3.3	11	3.35	
	14	4.1	10	2.47	
	15	5.9	7	1.20	
EG	16	8.5	6	0.71	0.95 ± 0.47
	17	2.4	4	1.65	
	18	2.9	3	1.04	
	19	7.8	3	0.38	
	20	7.2	7	0.97	

*, **: $p < 0.05, 0.01$ vs. Control group

Table 4 Spi$^-$ MFs in the livers of *gpt* delta rats treated with ES, MEG and EG for 4 weeks

Treatment	Animal No.	Plaques within XL-1 Blue MRA ($\times 10^5$)	Plaques within WL95 (P2)	Mutant frequency ($\times 10^{-5}$)	Mean±SD
Control	1	15.7	5	0.72	0.62 ± 0.13
	2	13.5	8	0.49	
	3	12.1	6	0.53	
	4	10.9	5	0.60	
	5	14.8	4	0.78	
ES	6	6.1	47	1.59	1.32 ± 0.48
	7	6.0	36	1.31	
	8	8.6	51	1.98	
	9	5.8	53	1.01	
	10	5.0	41	0.74	
MEG	11	6.7	3	2.22	1.30 ± 0.76
	12	9.5	16	1.67	
	13	8.4	4	0.22	
	14	4.3	3	1.45	
	15	3.9	3	0.95	
EG	16	8.1	7	0.58	0.52 ± 0.12
	17	9.8	5	0.33	
	18	9.1	5	0.64	
	19	9.5	4	0.56	
	20	13.3	2	0.51	

Table 5 *gpt* MFs in the kidneys of *gpt* delta rats treated with ES, MEG and EG for 4 weeks

Treatment	Animal No.	Cm^R colonies ($\times 10^5$)	6-TG^R and Cm^R colonies	Mutant frequency ($\times 10^{-5}$)	Mean ± SD
Control	1	7.4	8	1.08	1.07 ± 0.40
	2	8.2	6	0.73	
	3	8.0	14	1.75	
	4	2.3	2	0.85	
	5	3.2	3	0.94	
ES	6	4.6	10	2.18	0.85 ± 0.77
	7	5.1	3	0.59	
	8	10.9	6	0.55	
	9	5.7	4	0.71	
	10	4.6	1	0.22	
MEG	11	11.1	7	0.63	0.67 ± 0.67
	12	3.6	1	0.28	
	13	9.5	6	0.63	
	14	12.6	7	0.56	
	15	6.4	8	1.25	
EG	16	2.3	3	1.28	1.45 ± 0.54
	17	6.3	13	2.05	
	18	4.9	7	1.44	
	19	2.2	4	1.81	
	20	3.1	2	0.65	

Table 6 Spi⁻ MFs in the kidneys of *gpt* delta rats treated with ES, MEG and EG for 4 weeks

Treatment	Animal No.	Plaques within XL-1 Blue MRA ($\times 10^5$)	Plaques within WL95 (P2)	Mutant frequency ($\times 10^{-5}$)	Mean ± SD
Control	1	12.7	4	0.32	0.53 ± 0.32
	2	15.1	9	0.60	
	3	11.5	11	0.95	
	4	7.7	1	0.13	
	5	4.6	3	0.65	
ES	6	5.3	1	0.19	0.28 ± 0.11
	7	10.7	4	0.37	
	8	12.0	2	0.17	
	9	7.5	2	0.27	
	10	7.1	3	0.42	
MEG	11	14.9	7	0.47	0.52 ± 0.27
	12	5.6	4	0.72	
	13	10.7	9	0.84	
	14	13.1	2	0.15	
	15	7.5	3	0.40	
EG	16	7.8	7	0.32	0.52 ± 0.31
	17	9.6	5	0.60	
	18	6.5	3	0.95	
	19	5.0	3	0.13	
	20	8.2	2	0.60	

別紙４

研究成果の刊行に関する一覧表

書籍

著者氏名	論文タイトル名	書籍全体の編集者名	書　籍　名	出版社名	出版地	出版年	ページ
	該当なし						

雑誌

発表者氏名	論文タイトル名	発表誌名	巻号	ページ	出版年
Ishii, Y., Takasu, S., Kuroda, K., Matsushita, K., Kijima, A., Nohmi, T., Ogawa, K., Umemura, T.	Combined application of comprehensive analysis for DNA modification and reporter gene mutation assay to evaluate kidneys of *gpt* delta rats given madder color or its constituents.	Anal. Bioanal. Chem.	406	2467-2475	2014

Anal Bioanal Chem (2014) 406:2467–2475
DOI 10.1007/s00216-014-7621-2

RESEARCH PAPER

Combined application of comprehensive analysis for DNA modification and reporter gene mutation assay to evaluate kidneys of *gpt* delta rats given madder color or its constituents

Yuji Ishii · Shinji Takasu · Ken Kuroda · Kohei Matsushita · Aki Kijima · Takehiko Nohmi · Kumiko Ogawa · Takashi Umemura

Received: 13 November 2013 / Revised: 7 January 2014 / Accepted: 9 January 2014 / Published online: 4 February 2014

Abstract DNA adductome analysis using liquid chromatography–tandem mass spectrometry is a promising tool to exhaustively search DNA modifications. Given that the molecular weight of chemical-specific adducts is determined by the total molecular weights of the active form and nucleotide bases, we developed a new method of comprehensive analysis for chemical-specific DNA adducts based on the principle of adductome analysis. The actual analytical mass range was 50 mass units up or down from the average molecular weight of the four DNA bases plus the molecular weight of the expected active form of the chemical. Using lucidin-3-*O*-primeveroside (LuP), lucidin-modified bases formed by its active form were exhaustively searched using this new method. Various DNA adducts, including Luc-N^2-dG and Luc-N^6-dA, were identified in the kidneys of rats given LuP. Together with measurement of 8-hydroxydeoxyguanosine (8-OHdG) levels, the combined application of this new method with a reporter gene mutation assay was performed to clarify renal carcinogenesis induced by madder color (MC) that includes LuP and alizarin (Alz) as constituent agents. A DNA adductome map derived from MC-treated rats was almost identical to that of LuP-treated rats, but not Alz-treated rats. Although 8-OHdG levels were elevated in MC- and Alz-treated rats, significant increases in *gpt* and Spi$^-$ mutant frequencies were observed only in MC- and LuP-treated rats. In addition, the spectrum of *gpt* mutants in MC-treated rats showed almost the same pattern as those in LuP-treated rats. The overall data suggest that LuP may be responsible for MC-induced carcinogenicity and that the proposed methodology is appropriate for exploring and understanding mechanisms of chemical carcinogenesis.

Keywords DNA adduct · Oxidative DNA damage · *gpt* delta · In vivo mutagenicity · Madder color

Introduction

Chemical carcinogenesis is believed to occur through multistage processes that occur in response to the sequential accumulation of gene mutations [1]. Therefore, clarification of gene mutations that arise during the early stages of chemical-induced carcinogenesis would be a promising strategy for understanding the primary effects of a given chemical. Recently, an in vivo mutation assay using *gpt* delta rodents was developed that takes into account the absorption, distribution, metabolism, and excretion of exogenous chemicals [2]. This method represents a promising tool for estimating the status of gene mutations that occur during the early stages of carcinogenesis [3–5]. While gene mutations are caused by several events such as topoisomerase inhibition [6] and disruption of DNA repair systems [7, 8], modification of nucleotide bases, such as chemical-specific bulky adducts [9, 10] and oxidized and alkylated DNA bases [11–14], have been considered to be main causes. Thus, in addition to data from reporter gene mutations, global information concerning chemical-specific DNA modifications is necessary for a better understanding of chemical carcinogenesis.

Electronic supplementary material The online version of this article (doi:10.1007/s00216-014-7621-2) contains supplementary material, which is available to authorized users.

Y. Ishii · S. Takasu · K. Kuroda · K. Matsushita · A. Kijima · K. Ogawa · T. Umemura (✉)
Division of Pathology, National Institute of Health Sciences, 1-18-1 Kamiyoga, Setagaya-ku, Tokyo 158-8501, Japan
e-mail: umemura@nihs.go.jp

T. Nohmi
Biological Safety Research Center, National Institute of Health Science, 1-178-1 Kamiyoga, Setagaya-ku, Tokyo 158-8501, Japan

Reactive metabolites of genotoxic carcinogens are generally able to bind to any DNA base at several positions. In the case of the heterocyclic amine 2-amino-3-methylimidazo[4,5-*f*]quinoline (IQ), an IQ-dG adduct at the C8 position is a well-known major DNA modification [15], while IQ-dG adducts at the N^2- or N7-positions [16, 17] and IQ-dA adducts at the N^6-position [17] have also been found. Recently, Kanaly et al. [18] proposed a new approach to complete an exhaustive survey of DNA adducts using liquid chromatography–tandem mass spectrometry (LC–MS/MS), i.e., DNA adductome analysis. This method was developed based on the principle that DNA adducts are prone to lose deoxyribose during the fragmentation process. Consequently, fragment ion peaks showing a loss of deoxyribose $[M+H-116]^+$ from the precursor ion $[M+H]^+$ in the MS spectrum may be presumed to be derived from DNA adducts. We therefore attempted to apply this principle to a comprehensive analysis of chemical-specific DNA adducts. In our new method, we performed a limited comprehensive analysis within a range around the mean value (247.0) of the four DNA base molecular weights plus the molecular weight of the active form of the corresponding chemical. The constitutive DNA base of each adduct can then be identified by further MS spectrum analysis. Given that mutations such as base substitutions and deletions in a *gpt* mutant colony can also be identified, this information may define a clear relationship between DNA base modifications and resulting gene mutations.

Madder color (MC), a dye and a food additive used in a variety of foods and drinks, is a potent carcinogen that in rats targets the kidneys and livers [19]. MC is composed of naturally occurring anthraquinone compounds such as alizarin (Alz) and lucidin-3-*O*-primeveroside (LuP) [20]. However, whether genotoxic mechanisms are involved in MC carcinogenesis and whether these constituents are responsible for MC-induced carcinogenicity remain unclear. We previously demonstrated that LuP was capable of forming Luc-specific DNA adducts in the kidneys and livers of rats and identified the precise chemical structures of two Luc-specific DNA adducts, Luc-N^2-dG and Luc-N^6-dA [21]. In addition, Alz treatment elevated levels of 8-hydroxydeoxyguanosine (8-OHdG), a marker of oxidatively damaged DNA, in rat kidney [22]. Here, a comprehensive analysis of chemical-specific DNA adducts was applied to kidneys of *gpt* delta rats treated with LuP, which confirmed that the Luc-specific DNA adducts described above were detectable. A comparison of data concerning DNA adducts, 8-OHdG levels, and reporter gene mutations in kidneys of *gpt* delta rats treated with MC to those treated with LuP or Alz was then performed to clarify the mechanisms of MC carcinogenesis.

Materials and methods

Chemicals and reagents

MC prepared according to the voluntary specification for preparation of MC as a food additive was obtained from the Japan Food Additives Association (Tokyo, Japan). In brief, MC was prepared from powdered madder root by extraction with 50 % ethanol, followed by concentration, filtration, addition of dextrin (30 % in total), spray-drying, mixing, and pulverization. LuP was extracted from MC (powder of *Rubia tinctorum* L. roots) used in Japan as a food coloring (San-Ei Gen. F.F.I., Inc., Osaka, Japan). Alz and alkaline phosphatase were purchased from Sigma-Aldrich Japan (St. Louis, MO, USA). Nuclease P1 was obtained from Wako Pure Chemical Industries, Ltd. (Osaka, Japan). The purities of Alz and LuP were 97 and 90.5 %, respectively, and their chemical structures are shown in Fig. 1.

Animal and treatments

The protocol for this study was approved by the Animal Care and Utilization Committee of the National Institute of Health Sciences (Tokyo). Five-week-old male F344 *gpt* delta rats carrying approximately 10 tandem copies of the transgene lambda EG10 per haploid genome were obtained from Japan SLC (Shizuoka, Japan). Twenty *gpt* delta rats were housed in polycarbonate cages (five rats per cage) with hardwood chips for bedding. The cages were maintained at a conventional temperature (23±2 °C), humidity (55±5 %), air change (12 times/h), and lighting (12 h light/dark cycle) and were given free access to a CRF-1 basal diet (Oriental Yeast Co., Ltd, Tokyo, Japan) and tap water. Starting at 6 weeks of age, the rats were fed for 8 weeks a diet containing 5.0 % (*w/w*) MC, 0.08 % (*w/w*) Alz, or 0.3 % (*w/w*) LuP or maintained as untreated controls. The dose of MC used was reported to be carcinogenic in an 18-month carcinogenicity study [19]. The Alz and LuP doses were calculated based on their concentration in MC. All rats were sacrificed at 8 weeks by exsanguination under isoflurane anesthesia, and the kidneys were immediately removed and weighed. The kidneys were frozen with liquid nitrogen and stored at −80 °C until measurement of chemical-specific DNA adducts and 8-OHdG in nuclear DNA, or evaluation in in vivo mutation assays.

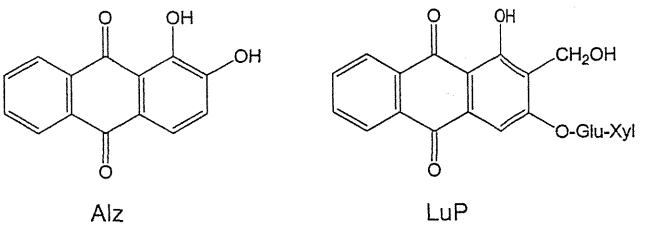

Fig. 1 Chemical structure of MC components

DNA extraction and digestion for comprehensive analysis of chemical-specific DNA adducts

DNA extraction and digestion was performed using a method that was slightly modified from that described in our previous report [23]. The samples were homogenized with lysis buffer included in the DNA Extractor® WB kit (Wako Pure Chemicals Industries, Ltd.). The mixture was centrifuged at 10,000×*g* for 1 min at 4 °C, and the pellet was dissolved in 200 μL enzyme reaction buffer. After treatment with RNase and protease K, the DNA pellet was obtained by washing with 2-propanol and ethanol, and centrifugation. The dried DNA pellet was dissolved in 100 μL water. The DNA concentration was analyzed using a NanoDrop ND-1000 UV–Vis spectrophotometer (Thermo Fisher Scientific Inc., Sunnyvale, CA, USA) and adjusted to 300 μg/450 μL. Then, 60 μL sodium acetate buffer, pH 4.8, was added and incubated with nuclease P1 (2,000 U/mL) at 37 °C for 3 h. After incubation, 60 μL 1.0 M Tris–HCl buffer, pH 8.2, was added and incubated with alkaline phosphatase (2,500 U/mL) at 37 °C for 3 h. The digested samples were passed through a 100,000 NMWL filter (Millipore, Bedford, MA, USA) and evaporated in a test tube. Methanol (1 mL) was then added to the test tube and the insoluble materials removed by centrifugation. After evaporation, the dried samples were stored at −80 °C and redissolved in 150 μL 30 % DMSO before LC–MS/MS analysis.

Comprehensive analysis of chemical-specific DNA adducts

LC–electron spray ionization (ESI)/MS/MS analyses were performed using a Quattro Ultima (Micromass, Beverly, MA, USA) coupled to a Hewlett Packard 1100 series (G1322A, degasser; G1312A, Bin Pump; G1316A, Colcom; G1329A, ALS; Agilent Technologies, Palo Alto, CA, USA). An aliquot (10 μL) of the sample was injected into a Wakosil-II C18 column (2.0×150 mm, 5 μm; Wako Pure Chemicals, Tokyo, Japan) that was maintained at 40 °C. Solvent A was 0.001 % formic acid, and solvent B was 0.001 % formic acid containing acetonitrile. The column was equilibrated with a mixture of solvent A/solvent B (95:5, *v/v*). A linear gradient was applied from 5 to 90 % acetonitrile over 0 to 30 min, kept at 90 % for 10 min, lowered to 5 % over 1 min, and equilibrated to the initial conditions for 14 min. The total run time was 45 min.

The mass spectrometer was operated using an ESI source in the positive ion mode (ESI^+) for multiple reaction monitoring (MRM). The cone voltage was 35 V, and the collision energy was 15 eV. The source block and desolvation temperatures were 150 and 400 °C, respectively. The cone gas flow rate was set at 200 L/h, and the desolvation gas was 600 L/h. According to the molecular weight of the expected active form of the chemicals and analytical mass range for the control, LuP, Alz, and MC-treated groups were set at *m/z* 437>321 to 567>451, *m/z* 467>351 to 567>451, *m/z* 437>321 to 537>421, and *m/z* 467>351 to 567>451, respectively.

Quantification of Luc-N^2-dG and Luc-N^6-dA adducts

The levels of Luc-N^2-dG and N^6-dA in the kidneys were quantified with our newly established isotope dilution method using LC–MS/MS [23]. LC–MS/MS analysis was performed using a Quattro Ultima coupled to a HEWLETT PACKARD 1100 series HPLC system. The mass spectrometer was operated using an ESI source in the positive ion mode (ES^+) for MRM. In the assay for Luc-N^2-dG, the precursor ion $[M+H]^+$ had a mass of *m/z* 520, and the selected product ion $[M+H\text{-glycoside-}252]^+$ had a mass of *m/z* 152. Correspondingly for $^{15}N_5$-Luc-N^2-dG, the precursor ion had a mass of *m/z* 525 and the selected product ion a mass of *m/z* 157. The cone voltage used was 14 V, and the collision energy was 14 eV. In the assay for Luc-N^6-dA, the precursor ion $[M+H]^+$ had a mass of *m/z* 509, and the selected product ion $[M+H\text{-glycoside}]^+$ had a mass of *m/z* 388. For $^{15}N_5$-Luc-N^6-dA, the precursor ion had a mass of *m/z* 509 and the selected product ion a mass of *m/z* 393. The cone voltage used was 12 V, and the collision energy was 18 eV. The amount of Luc-N^2-dG and Luc-N^6-dA was calculated as Luc-N^2-dG/10^8dG and Luc-N^6-dA/10^8dA, respectively.

DNA extraction and digestion for 8-OHdG analysis

DNA extraction was performed as described in the previous section. DNA digestion was performed according to the method of Tasaki et al. [24]. The dried DNA pellets were digested by an 8-OHdG assay preparation reagent set (Wako Pure Chemical Industries, Ltd.). Briefly, DNA pellets were dissolved in 150 μL DEPC water. After addition of 20 μL sodium acetate buffer, samples were incubated with nuclease P1 (2,000 U/mL) at 37 °C for 30 min. Then, 20 μL 1.0 M Tris–HCl buffer, pH 8.2, was added and incubated with alkaline phosphatase (2,500 U/mL) at 37 °C for 30 min. The digested samples were passed through a 100,000 NMWL filter (Millipore, Bedford, MA, USA) and stored at −80 °C until LC-ECD analysis.

Measurement of nuclear 8-OHdG

8-OHdG and dG were determined according to the method of Tasaki et al. [24]. Briefly, an aliquot (50 μL) of the sample was injected into a Wakosil-II C18 column (2.0×150 mm, 5 μm; Wako Pure Chemical Industries, Ltd.) maintained at 30 °C. The column was equilibrated with a mixture of 10 mM sodium phosphate/methanol (92:8, *v/v*). The compounds were eluted isocratically at a flow rate of 1.0 mL/min. The wavelength of the UV detector was set at 250 nm for dG detection.

The electrochemical detector ESA Coulochem II (Chelmsford, MA, USA) was used with a guard cell (Model 5020; 350 mV) and an analytical cell (Model 5011; electrode 1, 150 mV; electrode 2; 300 mV). The amount of 8-OHdG was calculated as 8-OHdG/10^5 dG.

In vivo mutation assays

6-Thioguanine (6-TG) and Spi$^-$ selections were performed using the method of Nohmi et al. [2]. Briefly, genomic DNA was extracted from the kidneys and livers of *gpt* delta rats in each group, and lambda EG10 DNA (48 kb) was rescued as phages by in vitro packaging. For 6-TG selection, packaging phages were incubated with *Escherichia coli* YG6020, which expresses Cre recombinase, and converted to plasmids carrying genes encoding *gpt* and chloramphenicol acetyltransferase. Infected cells were mixed with molten soft agar and poured onto agar plates containing chloramphenicol and 6-TG. The plates were then incubated at 37 °C for selection of 6-TG-resistant colonies, and *gpt* mutation frequency (MF) was calculated by dividing the number of *gpt* mutants after clonal correction with the number of rescued phages. *Gpt* mutations were characterized by amplifying a 739-bp DNA fragment containing the 456-bp coding region of the *gpt* gene and sequencing the PCR products with an Applied Biosystems 3730xl DNA Analyzer. For Spi$^-$ selection, packaged phages were incubated with *E. coli* XL-1 Blue MRA for survival titration and *E. coli* XL-1 Blue MRA P2 for mutant selection. Infected cells were mixed with molten lambda-trypticase agar plates. The next day, plaques (Spi$^-$ candidates) were punched out with sterilized glass pipettes and the agar plugs suspended in SM buffer. The Spi$^-$ phenotype was confirmed by spotting the suspensions on three types of plates where XL-1 Blue MRA, XL-1 Blue MRA P2, or the WL95 P2 strain was spread with soft agar. Spi$^-$ mutants, which produced clear plaques on every plate, were counted. Positive DNA samples (controls) were simultaneously applied in all in vivo mutation assays.

Statistical evaluation

The significance of differences in the results for body and kidney weight, 8-OHdG levels, and *gpt* and Spi$^-$ MFs was evaluated with Tukey's test.

Results

Body and kidney weights

Data for final body and kidney weights in *gpt* delta rats given MC, Alz, and LuP are shown in Table S1, electronic supplementary material. The body weights of rats in the MC- and Alz-treated groups were significantly lower than those fed the basal diet. Although changes in kidney weights of the treated rats were not observed, the relative kidney weights of rats in the MC-, LuP-, and Alz-treated group were significantly increased as compared to those fed the basal diet.

Confirmation of comprehensive analysis for chemical-specific DNA adducts detected by LC–MS/MS

To confirm the usefulness of a limited comprehensive analysis for chemical-specific DNA adducts, DNA adduct formation in the kidneys of rats treated with LuP was examined in the range of *m/z* 467 to 567, which was selected from the mean value of the molecular weight of the four DNA bases (247.0) plus that of Luc (270.2). The results from this comprehensive DNA adduct analysis are shown in Fig. 2. Several spots indicating putative DNA adducts derived from LuP-treatment were detected at *m/z* 520, 504, 502, and 480. Representative MRM chromatograms at *m/z* 520>404, 504>398, 502>396, and 480>364 of kidneys from LuP-treated rats are shown in Fig. 3. To examine the details of the adduct chemical structure, mass spectrum analyses were performed using the same samples. The product ion spectra of the *m/z* 520 and 504 of peaks I and IV when the collision energy was set at 5 and 20 eV are shown in Fig. S1 (electronic supplementary material). Characteristic product ions corresponding to glycoside bond cleavage, 1, 3-dihydroxy-2-methylanthraquinone, and nucleotides were clearly observed. In addition, the retention times (tR) of peaks I and IV corresponded to those of Luc-N^2-dG (*m/z* 520, tR 18.4 min) and Luc-N^6-dA (*m/z* 504, tR 22.6 min) standards, respectively, which were previously identified

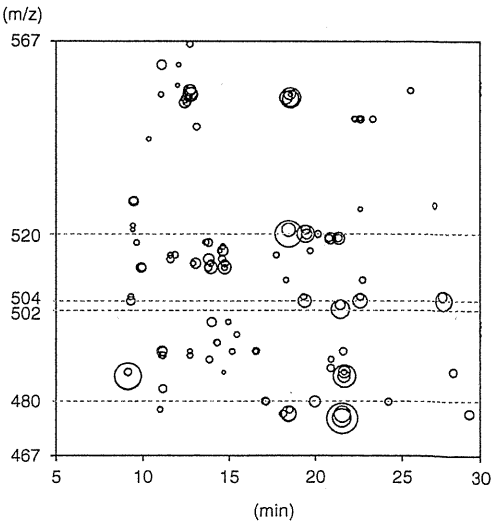

Fig. 2 DNA adductome map of kidneys from F344 *gpt* delta rats in the control and LuP-treated groups. The *X*-axis indicates peak retention time while the *Y*-axis indicates the mass-to-charge ratio. The spot size represents the peak area of the MRM chromatogram at $[M+H]^+>[M+H-116]^+$ in the mass range from *m/z* 467 to 567. The peaks detected in control and LuP-treated rats are represented as *black* and *blue spots*, respectively

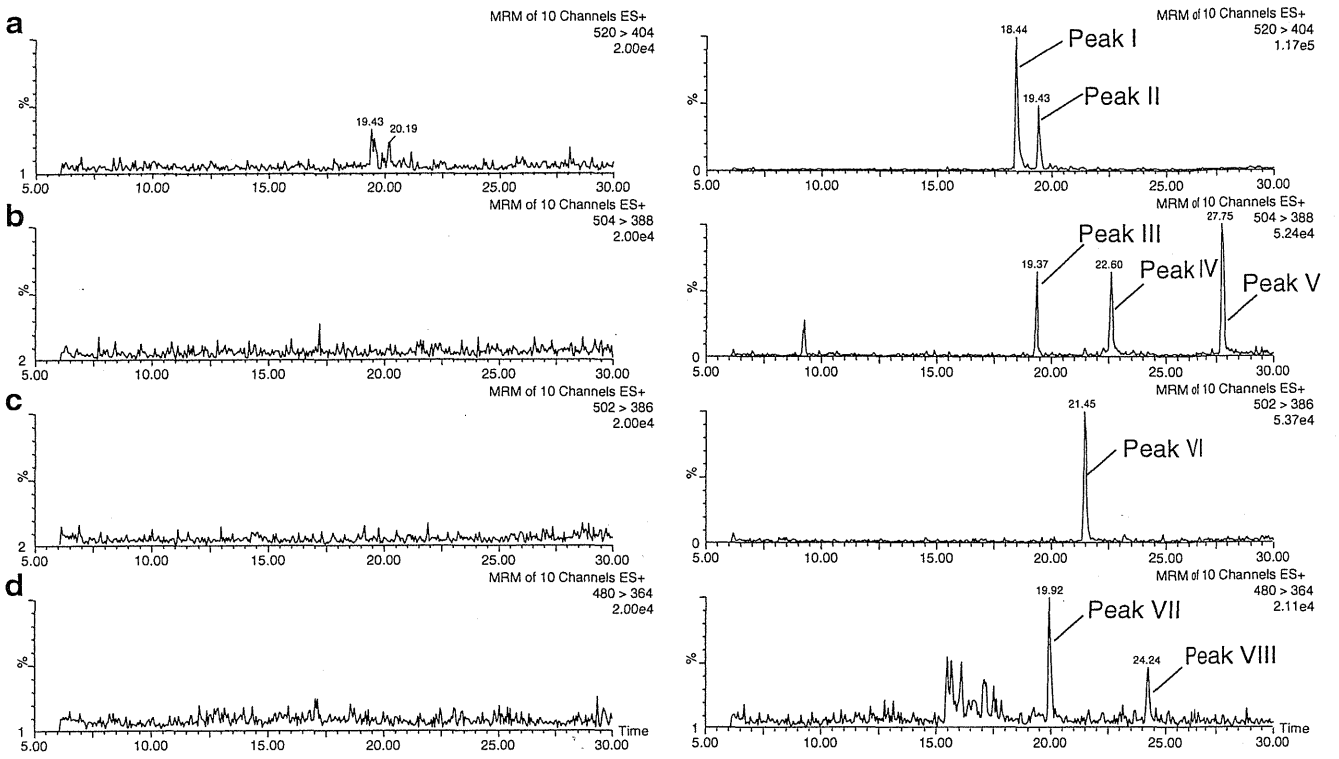

Fig. 3 Representative MRM chromatograms at *m/z* 520>404 (**a**), 504>398 (**b**), 502>396 (**c**), and 480>364 (**d**) in kidneys from F344 *gpt*delta rats in the control (*left*) and LuP-treated (*right*) groups. Eight putative DNA adduct peaks (I~VIII) were detected in LuP-treated rats

Luc-specific DNA adducts [21]. In the product ion spectra of $[M+H]^+$ ions, *m/z* 520, peak II, some product ions were observed, namely those at *m/z* 404 and 152, which could be attributed to a Luc-guanine adduct that arises following glycoside bond cleavage and guanine (Fig. S2, electronic supplementary material). Correspondingly, in the product ion spectra of the $[M+H]^+$ ions (*m/z* 504) of peaks III and V, some product ions, *m/z* 388, 252, and 136, were attributable to Luc-adenine adducts formed following glycoside bond cleavage, while 1 3-dihydroxy-2-methylanthraquinone and adenine were also observed (Fig. S3, electronic supplementary material). Therefore, these results indicate that these three peaks were Luc-modified dG and dA adducts, which are isomers of Luc-N^2-dG and N^6-dA. In addition, peaks VII and VIII detected at *m/z* 480 corresponded to the molecular ion of Luc-modified dC. In the product ion spectra of the $[M+H]^+$ ions (*m/z* 480), characteristic product ions *m/z* 364, 252, and 228 arose from Luc-cytosine adducts produced following glycoside bond cleavage, with 1, 3-dihydroxy-2-methylanthraquinone and deoxycytidine also observed (Fig. S4, electronic supplementary material). Although peak VI detected at *m/z* 502 did not correspond to molecular ions of representative Luc-modified bases, the product ions, *m/z* 386, were observable and could be attributed to modified bases formed following glycoside bond cleavage (Fig. S5, electronic supplementary material). Thus, peak VI is also considered to be one of the specific adducts derived from LuP treatment. The detected peak molecular ion (*m/z*), tRs, normalized peak areas, and identified or presumed DNA adducts obtained from the DNA adductome maps are summarized in Table 1.

Comprehensive analysis of chemical-specific DNA adducts in kidneys from MC- or Alz-treated rats

Chemical-specific DNA adduct formation in the kidneys of rats treated with Alz was examined in the range of *m/z* 437 to 537, which was selected from the mean value of the four DNA base molecular weights (247.0) plus that of Alz (240.2). The results from the comprehensive DNA adduct analysis are summarized in Fig. 4a. Kidneys from Alz-treated rats produced a DNA adductome map where the distribution and size of the spots were almost identical to those obtained with the

Table 1 Summary of putative DNA adducts detected in kidneys from F344 *gpt* delta rats treated with LuP for 8 weeks

Peak no.	*m/z*	Retention time (min)	Peak area	Presumed adducts
I	520	18.4	7,134	Luc-N^2-dG
II	520	19.4	2,488	Luc-modified dG
III	504	19.3	2,488	Luc-modified dA
IV	504	22.6	2,352	Luc-N^6-dA
V	504	27.8	6,774	Luc-modified dA
VI	502	21.5	4,083	Unknown adduct
VII	480	20.0	2,243	Luc-modified dC
VIII	480	24.2	841	Luc-modified dC

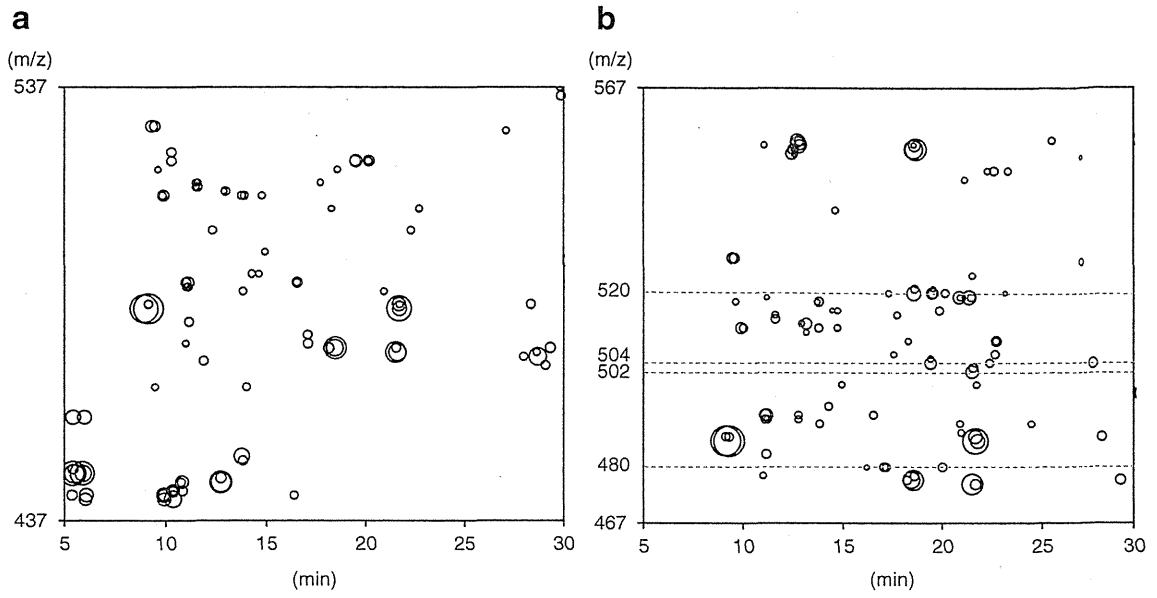

Fig. 4 DNA adductome map of kidneys from F344 *gpt* delta rats in the Alz- (**a**) and MC- (**b**) treated groups. The peaks detected in the control are represented as *black spots*, and the peaks detected in LuP- or MC-treated rats are represented as *blue spots*

control such that characteristic spots derived from Alz treatment were not observed. To confirm whether Luc-specific DNA adduct formation occurred, a comprehensive analysis of kidneys from MC-treated rats was performed in the range of *m/z* 467 to 567. In this DNA adductome map, some spots indicating DNA adduct formation were indeed detected (Fig. 4b). Meanwhile, the distribution and size of spots obtained from kidneys of rats treated with MC were almost identical to those treated with its genotoxic component LuP.

Quantitative analysis of Luc-specific DNA adducts

The quantitative levels of Luc-N^2-dG and Luc-N^6-dA indicated in peaks I and IV arising from kidneys from rats treated with LuP for 8 weeks are shown in Fig. S6 (electronic supplementary material). The Luc-N^2-dG/10^8dG ratios in the LuP- and MC-treated rats were 55.4 and 21.0, respectively, while the Luc-N^6-dA/10^8dA ratios were 3.9 and 2.6, respectively. These adducts were not detected in rats from the control and Alz-treated groups.

Oxidative DNA damage in kidneys

The 8-OHdG levels in kidneys after 8 weeks of MC, LuP, and Alz exposure are shown in Fig. S7 (electronic supplementary material). Significant increases ($p<0.01$) in 8-OHdG levels were observed in kidneys (1.66±0.68) from the Alz-treated group compared to the control group (0.32±0.07) and were three-fold higher (1.03±0.69) than the control in the MC-treated group. In contrast, there were no changes in 8-OHdG levels for the LuP-treated group.

In vivo mutation assays in kidneys

Data for *gpt* and Spi$^-$ MFs in the kidneys of *gpt* delta rats treated for 8 weeks with MC, LuP, or Alz are summarized in Tables 2, 3, and 4. Significant differences ($p<0.01$) in *gpt* MF were observed in MC- and LuP-treated groups (MC 2.72± 0.52, LuP 2.97±0.55) compared with the control group (0.37 ±0.21) (Table 2). To characterize the *gpt* mutations due to MC and LuP exposure, mutant colonies were analyzed by DNA sequencing (Table 3). In MC- and LuP-treated rats, A/T mutations predominated and accounted for 50.8 % (94/185) and 52.9 % (72/136) of the mutations, respectively. The specific mutation frequencies of AT-TA transversions ($p<0.01$), AT-GC transitions ($p<0.01$), and GC-TA transversions ($p<0.05$) in MC- and LuP-treated groups were significantly higher than for the control group. As shown in Table 4, Spi$^-$ MFs also significantly increased in the MC- and LuP-treated groups (MC 1.72±0.38, LuP 1.69±0.75) compared with the control group (0.58±0.17). However, there were no significant differences in either *gpt* or Spi$^-$ MFs in Alz-treated rats.

Discussion

Taking advantage of the fact that glycoside bonds are subject to cleavage when DNA bases are modified with bulky adducts, we developed a new method for comprehensively analyzing for chemical-induced bulky DNA adducts. According to a DNA adductome analysis established by Kanaly et al. [18], fragment ions with loss of deoxyribose from the precursor ion on a MS spectrum are likely derived from DNA

Table 2 *Gpt* mutation frequencies in kidneys from *gpt* delta rats treated for 8 weeks with MC, LuP, and Alz

Site	Kidney				
Treatment	Animal no.	Cm^R colonies ($\times 10^5$)	6-TG^R and Cm^R colonies	Mutant frequency ($\times 10^{-5}$)	Mean±SD
Basal diet	1	10.5	1	0.10	0.37±0.21
	2	7.4	5	0.68	
	3	7.4	3	0.41	
	4	11.2	3	0.27	
	5	10.5	4	0.38	
MC	6	14.2	27	1.90	2.72±0.52*
	7	12.2	40	3.29	
	8	14.9	45	3.01	
	9	14.9	40	2.69	
	10	12.1	33	2.74	
LuP	11	7.6	23	3.04	2.97±0.55*
	12	8.0	27	3.37	
	13	11.8	24	2.03	
	14	9.0	30	3.35	
	15	10.4	32	3.08	
Alz	16	6.4	9	1.40	0.69±0.54
	17	12.7	5	0.39	
	18	19.1	3	0.16	
	19	9.9	8	0.81	
	20	13.0	8	0.62	

*$p<0.01$ vs. basal diet

adducts. We therefore expected that precursor ions having a mass either 50 mass units higher or lower than the average molecular weight of the four DNA bases plus the molecular weight of the expected active form of the chemical where the fragment ion lost the deoxyribose from the precursor ion may originate from chemical-specific DNA adducts. In the present study, we confirmed adduct formation using LuP wherein DNA adducts were identified as N^2-guanine and N^6-adenine substitutions [21]. Since the average molecular weights of the four DNA bases and Luc were 247.0 and 270.2, respectively, the fragment ion $[M+H-116]^+$ from the precursor ion $[M+H]^+$ was detected as eight spots of varying sizes in the mass range from *m/z* 467 to 567. Qualitative analysis using chemically synthesized standards led to the conclusion that two spots detected at *m/z* 520 at 17 min and *m/z* 504 at 22 min were Luc-N^2-dG and Luc-N^6-dA, respectively. Subsequently, to confirm whether the remaining six spots were derived from Luc-specific DNA adducts, analyses of the product ion spectrum were performed at *m/z* 520 (one spot), 504 (two spots), 502 (one spot), and 480 (two spots). The spectrum showed that five of six spots detected at *m/z* 520, 504, and 480 originated from Luc-modified dG, dA, and dC, respectively. With respect to the remaining spot at *m/z* 502, no DNA base could be identified due to the low product ion yield. Thus, the overall data suggest that our new method based on the concept

Table 3 Mutation spectra in the kidneys of *gpt* delta rats treated for 8 weeks with MC, LuP, or Alz

	Control	MC	LuP	Alz
Base substitution				
Transversion				
GC-TA	–	0.40±0.09*	0.37±0.25*	0.13±0.12
GC-CG	–	0.15±0.07	0.33±0.28	0.03±0.07
AT-TA	0.07±0.07	0.83±0.18**	0.91±0.19**	0.08±0.14
AT-CG	0.03±0.06	0.09±0.09	0.12±0.19	0.02±0.03
Transition				
GC-AT	0.14±0.10	0.36±0.26	0.30±0.21	0.19±0.16
AT-GC	0.04±0.06	0.45±0.19**	0.53±0.16**	0.07±0.06
Deletion				
Single bp	0.04±0.05	0.14±0.14	0.11±0.08	0.15±0.15
Over 2 bp	0.03±0.06	0.05±0.07	0.05±0.17	–
Insertion	–	0.07±0.08	0.13±0.11	–
Complex	0.02±0.04	0.19±0.09	0.12±0.15	–

*$p<0.05$ vs. control group; **$p<0.01$ vs. control group

Table 4 Spi^- mutant frequencies in kidneys from F344 *gpt* delta rats treated for 8 weeks with MC, LuP, or Alz

Treatment	Animal no.	Plagues within XL-1 Blue MRA ($X10^5$)	Plagues within WL95 (P2)	Mutant frequency ($\times 10^{-5}$)	Mean±SD
Basal diet	1	13.3	10	0.75	0.75±0.03
	2	14.9	11	0.74	
	3	11.4	9	0.79	
	4[a]	–	–	–	
	5	14.0	10	0.71	
MC	6	16.4	24	1.47	1.72±0.38*
	7	12.4	17	1.37	
	8	17.1	29	1.70	
	9	12.2	21	1.73	
	10	6.4	15	2.35	
LuP	11	7.7	17	2.20	1.69±0.75*
	12	8.6	7	0.81	
	13	7.6	11	1.46	
	14	8.5	11	1.30	
	15	9.3	25	2.70	
Alz	16	9.3	4	0.43	0.58±0.17
	17	10.2	6	0.59	
	18	4.8	2	0.42	
	19	9.4	6	0.64	
	20	9.6	8	0.83	

[a] The data were excluded for the calculation of the MF because of no detection of *gpt* mutant colony on the plate

*$p<0.05$ vs. control group

of adductome analysis would be a useful tool for making comprehensive surveys of chemical-specific DNA adducts.

To compare the adductome maps derived from MC- or Alz-induced DNA adducts with that of Luc-specific adducts, a comprehensive analysis for chemical-induced DNA adducts was performed on kidney DNA from rats treated for 8 weeks with diets supplemented with MC or Alz at concentrations of 5.0 and 0.8 %, respectively. The distribution and size of spots in the adductome map of MC-treated animals were almost identical to those of LuP. While the sizes of the spots do not always represent the amount of the comparable DNA adducts due to the lack of cone voltage optimization for each DNA adduct, in so far as DNA adductome maps are compared under the same conditions, the distribution and spot sizes do reflect characteristics of the DNA adducts. Quantitative analysis by an isotope dilution LC–ESI–MS/MS method using SIR for presumably the same spots derived from Luc-N^2-dG and Luc-N^6-dA adducts in the maps of MC-treated and LuP-treated animals was performed. The putative two spots in MC-treated animals almost certainly have a respective Luc-N^2-dG and Luc-N^6-dA derivation, and their amounts were equivalent to those of LuP-treated rats. On the other hand, some spots detected in the adductome map of Alz-treated animals were almost identical to those of the control, which is in line with previous data showing that Alz had neither direct DNA damage nor mutagenicity potential [25, 26]. Thus, the comparison among the adduct maps allowed us to conclude that LuP is a potential candidate to contribute to MC-induced direct DNA damage. With respect to MC-induced oxidative stress, participation of the catechol structure in the Alz anthraquinone ring has been proposed. Inoue et al. [22] found that levels of 8-OHdG were increased in the kidney DNA of rats treated with MC or Alz. In the present study, exposure of *gpt* delta rats to Alz also clearly elevated 8-OHdG levels in the kidney DNA. Elevated 8-OHdG levels were also observed in MC-treated rats, albeit without statistical significance. Thus, our data suggest that Alz is a potential candidate agent to promote MC-induced DNA oxidation.

In the reporter gene mutation assay, *gpt* and Spi$^-$ MFs were significantly increased in kidneys of rats given MC for 8 weeks. This is the first report showing MC-induced in vivo mutagenicity. In addition to the data from the comprehensive survey for MC-induced bulky DNA adducts, the increased MF induced by MC strongly suggests involvement of genotoxic mechanisms in MC-induced renal carcinogenesis. Analysis of the mutation spectra in *gpt* mutants induced by MC treatment revealed significant increases in specific mutation frequencies of GC-TA, AT-TA transversions, and AT-GC transitions. Given that 8-OHdG primarily causes GC-TA transversion by causing A base mispairing during DNA replication [11], oxidative DNA damage might also play a key role in MC carcinogenicity. However, exposure of *gpt* delta rats to Alz, a possible contributor to MC-induced oxidative stress, did not elevate *gpt* and Spi$^-$ MFs, despite the ability of Alz to markedly increase 8-OHdG levels. Significant increases in GC-TA transversions were also observed in LuP-treated rats despite the finding that LuP had no potential for inducing oxidative DNA damage. Instead, in addition to well-matched DNA adductome maps between LuP- and MC-treated animals, the mutation frequencies of *gpt* and Spi$^-$ and spectra of *gpt* mutations in the kidneys of LuP-treated rats were almost identical to those produced by MC. Therefore, it is likely that the mechanisms underlying MC-induced mutagenicity might involve LuP-induced direct DNA damage, but not Alz-induced oxidative stress. Increases in A/T site mutations, including AT-TA transversions and AT-GC transitions, were prominent in LuP- and MC-treated groups along with a rise in G/C site mutations to a certain extent. The present comprehensive analysis for LuP- or MC-induced bulky adducts demonstrated the existence of two unknown isomers of Luc-modified dA adducts in addition to N^6-dA adducts. Accordingly, theses dA adducts might mainly contribute to MC-induced mutagenicity, although further examination will be necessary to clarify their genotoxic potential.

In conclusion, this new method for comprehensive analysis of chemical-induced bulky DNA adducts based on the principle of adductome analysis was established and validated by assessing LuP-modified bases as reported in our previous study. Applying this method together with a reporter gene mutation assay produced results that indicate that LuP may be the substance responsible for MC-induced carcinogenicity.

Acknowledgments This work was supported part by a Grant-in-Aid from the Ministry of Health, Labour and Welfare, Japan.

References

1. Weston A, Harris CC (2000) Holland-Frei cancer medicine, 5th edn. BC Decker, Canada
2. Nohmi T, Suzuki T, Masumura K (2000) Recent advances in the protocols of transgenic mouse mutation assays. Mutat Res 455:191–215
3. Suzuki Y, Umemura T, Hibi D, Inoue T, Jin M, Ishii Y, Sakai H, Nohmi T, Yanai T, Nishikawa A, Ogawa K (2012) Possible involvement of genotoxic mechanisms in estragole-induced hepatocarcinogenesis in rats. Arch Toxicol 86:1593–1601
4. Hibi D, Suzuki Y, Ishii Y, Jin M, Watanabe M, Sugita-Konishi Y, Yanai T, Nohmi T, Nishikawa A, Umemura T (2011) Site-specific in vivo mutagenicity in the kidney of gpt delta rats given a carcinogenic dose of ochratoxin A. Toxicol Sci 122:406-414
5. Jin M, Kijima A, Hibi D, Ishii Y, Takasu S, Matsushita K, Kuroda K, Nohmi T, Nishikawa A, Umemura T (2013) In vivo genotoxicity of methyleugenol in gpt delta transgenic rats following medium-term exposure. Toxicol Sci 131:387–394
6. Baguley BC, Ferguson LR (1998) Mutagenic properties of topoisomerase-targeted drugs. Biochem Biophys Acta 1400:213–222
7. Lagerqvist A, Håkansson D, Lundin C, Prochazka G, Dreij K, Segerbäck D, Jernström B, Törnqvist M, Frank H, Seidel A, Erixon

K, Jenssen D (2011) DNA repair and replication influence the number of mutations per adduct of polycyclic aromatic hydrocarbons in mammalian cells. DNA Repair 10:877–886
8. Alvi NK, Foiles PG, Williams GM (1990) Inhibition of repair of O6-methyldeoxguanosine and enhanced mutagenesis in rat-liver epithelial cells. Mutat Res 230:219–226
9. Seo KY, Nagalingam A, Tiffany M, Loechler EL (2005) Mutagenesis studies with four stereoisomeric N2-dG benzo[a]pyrene adducts in the identical 5′-CGC sequence used in NMR studies: G>T mutations dominate in each case. Mutagenesis 20:441–448
10. Zhao B, Wang J, Geacintow NE, Wang Z (2006) Poleta, Polzeta and Rev1 together are required for G to T transversion mutations induced by the (+)-and (−)-trans-anti-BPDE-N2-dG DNA adducts in yeast cells. Chem Res Toxicol 34:417–425
11. Cheng KC, Hahill DS, Kasai H, Nishimura S, Loeb LA (1992) 8-Hydroxyguanine, an abundant form of oxidative DNA damage, causes G-T and A-C substitutions. J Biol Chem 267:166–172
12. Kalam MA, Haraguchi K, Chandani S, Loechler EL, Moriya M, Greenberg MM, Basu AK (2006) Genetic effects of oxidative DNA damages: comparative mutagenesis of the imidazole ring-opened formamidopyrimidines (Fapy lesions) and 8-oxo-purines in simian kidney cells. Nucleic Acids Res 43:2305–2315
13. Shibata MA, Shirai T, Ogawa K, Takahashi S, Wild CP, Montesano R, Tsuda H, Ito N (1994) DNA methylation adduct formation and H-ras gene mutations in progression of *N*-buthyl-*N*-(4-hydroxybutyl)nitrosamine-induced bladder tumors caused by a single exposure to *N*-methyl-*N*-nitrosourea. Carcinogenesis 15:2965–2968
14. Hamid S, Eckert KA (2005) Effect of DNA polymerase beta loop variants on discrimination of O6-methyldeoxyguaosine modification present in the nucleotide versus template substrate. Biochemistry 44: 10378–10387
15. Snyderwine EG, Roller PP, Adamson RH, Sato S, Thorgeirsson SS (1988) Reaction of *N*-hydroxylamine and *N*-acetoxy derivatives of 2-amino-3-methylimidazolo[4,5-f]quinolone with DNA. Synthesis and identification of *N*-(deoxyguanosin-8-yl)-IQ. Carcinogenesis 9: 1061–1065
16. Turesky RJ, Markovic J, Aeschlimann JM (1996) Formation and differential removal of C-8 and N2-guanine adducts of the food carcinogen 2-amino-3-methylimidazo[4,5-f]quinolone in the liver, kidney, and colorectum of the rat. Chem Res Toxicol 9:397–402
17. Jamin EL, Arquier D, Canlet C, Rathahao E, Tulliez J, Debrauwer L (2007) New insights in the formation of deoxynucleoside adducts with the heterocyclic aromatic amines PhIP and IQ by means of ion trap MSn and accurate mass measurement of fragment ions. J Am Soc Mass Spectrom 18:2107–2118
18. Kanaly RA, Hanaoka T, Sugimura H, Toda H, Matsui S, Matsuda T (2006) Development of the adductome approach to detect DNA damage in humans. Antioxid Redox Signal 8:993–1001
19. Inoue K, Yoshida M, Takahashi M, Shibutani M, Takagi H, Hirose M, Nishikawa A (2009) Induction of kidney and liver cancers by the natural food additive madder color in a 2-year rat carcinogenicity study. Food Chem Toxicol 47:1400
20. Kawasaki Y, Goda Y, Yoshihira K (1992) The mutagenic constituents of *Rubia tinctorum*. Chem Pharm Bull 40:1504–1509
21. Ishii Y, Okamura T, Inoue T, Fukuhara K, Umemura T, Nishikawa A (2010) Chemical structure determination of DNA bases modified by active metabolites of lucidin-3-*O*-primeveroside. Chem Res Toxicol 23:134–141
22. Inoue K, Yoshida M, Takahashi M, Fujimoto H, Ohnishi K, Nakashima K, Shibutani M, Hirose M, Nishikawa A (2009) Possible contribution of rubiadin, a metabolite of madder color, to renal carcinogenesis in rats. Food Chem Toxicol 47:752–759
23. Ishii Y, Inoue K, Takasu S, Jin M, Matsushita K, Kuroda K, Fukuhara K, Nishikawa A, Umemura T (2012) Determination of lucidin-specific DNA adducts by liquid chromatography with tandem mass spectrometry in the livers and kidneys of rats given lucidin-3-*O*-primeveroside. Chem Res Toxicol 25:1112–1118
24. Tasaki M, Umemura T, Suzuki Y, Hibi D, Inoue T, Okamura T, Ishii Y, Maruyama S, Nohmi T, Nishikawa A (2010) Oxidative DNA damage and reporter gene mutation in the livers of gpt delta rats given non-genotoxic hepatocarcinogens with cytochrome P450-inducible potency. Cancer Sci 101:2525–2530
25. Poginsky B, Westendorf J, Blomeke B, Marquardt H, Hewer A, Grover PL, Phillips DH (1991) Evaluation of DNA-binding activity of hydroxyanthraquinones occurring in *Rubia tinctrum* L. Carcinogenesis 12:1265–1271
26. Kaur P, Chandel M, Kumar S, Kumar N, Kaur S (2010) Modulatory role of alizarin from *Rubia cordifolia* L. against genotoxicity of mutagens. Food Chem Toxicol 48:320–325